Coherent control of high-harmonic generation using waveform-synthesized chirped laser fields

Xu Wang, Cheng Jin, and C. D. Lin
Department of Physics, Kansas State University, Manhattan, Kansas 66506, USA
(Received 2 July 2014; revised manuscript received 21 August 2014; published 28 August 2014)

We show that waveform-synthesized chirped laser fields are efficient tools for coherent harmonic control. A single harmonic order, or two harmonic orders, can be selectively enhanced by using a two-color field allowing a moderate linear chirp for each color. Different harmonic orders within a wide spectral range can be selectively enhanced by adjusting the laser parameters. Our theory bridges two current harmonic control techniques, namely, single-color phase shaping and multicolor amplitude synthesis, and opens the door to new harmonic control possibilities.

DOI: 10.1103/PhysRevA.90.023416 PACS number(s): 32.80.Fb, 32.80.Rm

I. INTRODUCTION

High-harmonic generation (HHG) has been extensively studied during the past decade for its promise as light sources at extreme ultraviolet and soft-x-ray frequencies [1,2] and for its application in generating attosecond pulses [3–5]. Understanding and controlling the HHG process is the basis of enhancing the yields or manipulating the properties of the high-frequency light sources or the attosecond pulses.

Much work has been done in coherent control of HHG. Due to difficulties in manipulating directly a harmonic spectrum [6], which normally spans a broad frequency range from ultraviolet to soft x-ray, most current HHG control methods are instead relying on controlling the driving laser field before its interaction with the gas medium, where harmonics are generated.

There are two commonly used techniques of manipulating the driving laser field for the purpose of controlling the resulting harmonic generation. One is to shape the 800 nm femtosecond pulses generated from a Ti:sapphire laser in the frequency domain, which is divided into dozens of small components and the phases of individual components are adjusted [7–11]. This phase shaping can be combined with an adaptive learning loop [12] such that an optimal combination of the phase components can be found for a predetermined goal, such as to maximize the yield of a particular harmonic order or to maximize the contrast ratio between a target harmonic order and the neighboring orders. After phase shaping, a transform limited laser pulse is usually turned into a complicated and highly structured field without a simple analytical expression.

The other harmonic control technique makes use of one or more colors in addition to the fundamental [13–29]. By coherently synthesizing the field amplitudes, the subcycle field shape (or waveform) can be changed, therefore both the ionization and the subsequent electron motion can be steered. Commonly used additional colors include the second harmonic and the third harmonic of the fundamental due to experimental convenience [14–22], although other colors have also been widely explored [23–29]. This multicolor amplitude synthesis has led to substantial progress on coherent harmonic control towards various purposes, such as extending the harmonic cutoff, enhancing the HHG yield, generating an isolated attosecond pulse, etc.

It is therefore natural and interesting to ask whether these two harmonic control techniques, namely, "single-color" phase shaping and multicolor amplitude synthesis, can be combined to better control the harmonic generation process than either of them alone, at least for some harmonic control goals. To answer this question is the main goal of this paper. We will show that even the simplest version of this combination, a two-color field with each color linearly chirped, is capable of enhancing a single harmonic with selectivity and contrast superior to the existing phase shaping method. In addition, this simplest combination can also be used to achieve new harmonic control options that have not been reported in literature, such as selectively enhancing two harmonic orders of interest. Moreover, going one step further beyond the simplest combination by using a three-color field, we have obtained qualitative agreement to a recently published experiment that has not been fully understood [19].

Selective enhancement of a single harmonic has gained substantial interest in the past decade [7–11,19,20]. Almost all the works have been done using the phase shaping technique and gas-filled fibers [7–11]. It has been experimentally confirmed by at least two groups that using the phase shaping technique, single harmonic enhancement cannot be achieved using gas jets [6,9]. This implies that some spatial fiber modes must be exploited which greatly complicates the understanding of this process. Additionally, both the selectivity and the contrast are limited: The spectral region within which a single harmonic can be selectively enhanced is narrow and the contrast ratio between the target harmonic and its nearest neighbors is usually limited to two or three times [7,10]. These limitations are the consequences of the narrow bandwidth of an 800 nm field.

An exception was reported recently by Wei *et al.* [19]. By using a gas-jet setup and a three-color field [800 nm and its second and third harmonics generated from beta barium borate (BBO) crystals], a single harmonic can be selectively enhanced with an unprecedented contrast ratio of over ten times between the target order and its nearest neighbors. Different harmonic orders can be selectively enhanced by changing the laser parameters. The experimental results are promising, but the underlying physics requires further explanation, which will be given in this paper.

This paper is organized as follows. In Sec. II we will give an explanation of the method that we use to calculate harmonic spectra and a detailed search procedure for the laser parameters that yield a desired harmonic property. In Sec. III we will show the main numerical results and the corresponding physical analyses. In Sec. IV we will extend from two colors to three colors and connect to the experiment reported in [19]. In Sec. V a summary will be

given. Atomic units (a.u.) will be used unless otherwise specified.

II. THEORETICAL METHODS

A. Laser electric field

For the major part of this paper, we will be using a two-color laser field and allowing a linear chirp for each color. (In Sec. IV we will add a third color for the purpose of connecting to a recent experiment. The details of the laser electric field with three colors will be given then.) As mentioned in the previous section, this is the simplest version of combining single-color phase shaping and multicolor amplitude synthesis, the two commonly used harmonic control techniques. The resulting laser electric field has a simple analytical form given by

$$E(t) = \cos^2(\pi t/\tau)[E_1\cos(\omega_1 t + \alpha_1 t^2) + E_2\cos(\omega_2 t + \alpha_2 t^2 + \phi_2)], \quad (1)$$

where τ is the full duration of the cosine-square pulse envelope, E_i, ω_i, and α_i are the amplitude, angular frequency, and linear chirp rate of the ith field, respectively, with $i = 1$ for the 800 nm fundamental field and $i = 2$ for the additional field. We will use the third harmonic or the second harmonic of the fundamental field as the additional field, for the reason that these two harmonics can be easily obtained in experiments. We have set the carrier envelope phase (CEP) of the fundamental field to be zero, but the CEP of the additional field, ϕ_2, is allowed to change within $[0,2\pi]$. The two fields are polarized in parallel.

To reduce the number of free parameters in Eq. (1), we will use a pulse duration of ten laser cycles (full width at half maximum, FWHM), in terms of the fundamental field. This corresponds to a time of about 27 fs. This pulse duration is long enough to avoid any few-cycle characteristics, such as the dependence on the CEP of the fundamental field [30].

We will also fix the intensity ratio between the two fields. This is justified by the fact that in a real experiment, the efficiency of converting the fundamental field into its second or third harmonics is roughly fixed by the conversion apparatus, usually a BBO crystal. For example, the intensity conversion efficiency is shown to be about 15% for the second harmonic and about 5% for the third harmonic [19]. These two intensity ratios will be used in this paper.

Therefore for a given fundamental intensity, the laser electric field in Eq. (1) is characterized by the three parameters $(\alpha_1,\alpha_2,\phi_2)$. A harmonic spectrum with some desired property may be realized if the three parameters are properly combined. For example, we will show in later sections that a single harmonic order, or two harmonic orders of interest, can be selectively enhanced with proper laser parameter combinations.

There are now two questions: (1) Given a laser electric field with all the parameters specified, how do we calculate the harmonic spectrum? (2) How do we find the laser parameters that yield a harmonic spectrum of desired properties? These two questions will be answered in the following two sections.

B. The strong-field approximation

We calculate harmonic spectra using the strong-field approximation (SFA), or the so-called "Lewenstein model," the details of which have been elaborated in Ref. [31]. Here we only list a few key formulas for the completeness of the current paper. The time-dependent dipole moment, in vector form, is given by

$$\mathbf{x}(t) = i\int_{-\tau/2}^{t} dt' \int d^3\mathbf{p}\, \mathbf{d}^*[\mathbf{p} - \mathbf{A}(t')] \times \{\mathbf{E}(t')\cdot\mathbf{d}[\mathbf{p} - \mathbf{A}(t')]\}\exp[-iS(\mathbf{p},t,t')] + \text{c.c.}, \quad (2)$$

where t' is the time of electron emission, with all the previous times (from the beginning of the pulse at $-\tau/2$) included by the first integral; $\mathbf{p} = \mathbf{v} + \mathbf{A}(t)$ is a canonical momentum with $\mathbf{A}(t)$ being the vector potential of the laser field; $S(\mathbf{p},t,t')$ is the classical action accumulated by the electron from t' to the current time t:

$$S(\mathbf{p},t,t') = \int_{t'}^{t} dt''\left(\frac{[\mathbf{p} - \mathbf{A}(t'')]^2}{2} + I_p\right), \quad (3)$$

where I_p is the ionization potential of the target atom.

In this paper we will use the dipole transition matrix element for hydrogenlike atoms:

$$\mathbf{d}(\mathbf{v}) = i\left(\frac{2^{7/2}\alpha^{5/4}}{\pi}\right)\frac{\mathbf{v}}{(\mathbf{v}^2+\alpha)^3}, \quad (4)$$

which describes a transition from a ground state s wave function to a continuum state with kinetic momentum $\mathbf{v}$ or vice versa. Note that $\alpha = 2I_p$. In this paper we will use Ne and Ar as the target atoms, with $I_p = 0.79$ and 0.58 a.u., respectively.

The 3D momentum integration in Eq. (2) can be evaluated using a saddle-point approach and the result reads

$$\mathbf{x}(t) = i\int_{-\tau/2}^{t} dt'\left(\frac{\pi}{\varepsilon + i(t-t')/2}\right)^{3/2}\mathbf{d}^*[\mathbf{p}_s - \mathbf{A}(t')] \times \{\mathbf{E}(t')\cdot\mathbf{d}[(\mathbf{p}_s - \mathbf{A}(t')]\}\exp[-iS(\mathbf{p}_s,t,t')] + \text{c.c.}, \quad (5)$$

where ε is an infinitesimal regularization constant and

$$\mathbf{p}_s = \mathbf{p}_s(t,t') = \frac{1}{t-t'}\int_{t'}^{t} dt''\mathbf{A}(t'') \quad (6)$$

is the stationary momentum.

We use Eq. (5) to calculate the time-dependent dipole moment $\mathbf{x}(t)$ by doing the integration in time numerically. Then $\mathbf{x}(t)$ is Fourier transformed into the frequency domain

$$\tilde{\mathbf{x}}(\omega) = \int \mathbf{x}(t)e^{-i\omega t}dt. \quad (7)$$

What will be plotted in later sections as harmonic yield is the quantity $|\tilde{\mathbf{x}}(\omega)|^2\omega^4$, as a function of harmonic orders, in terms of the fundamental frequency.

We will explain in later sections that the physical effects that we are interested in, viz., selective enhancement of a single harmonic order, or two harmonic orders, are mainly the result of the external laser field, or of the "wave packet" from the concept of the quantitative rescattering theory [32], and the role of the atomic target is minor. So SFA calculations are sufficient for our purpose here.

C. Laser parameter search procedure

In this section we will explain how we search for a laser parameter combination $(\alpha_1,\alpha_2,\phi_2)$ that yields a high-harmonic spectrum with desired properties. For example,

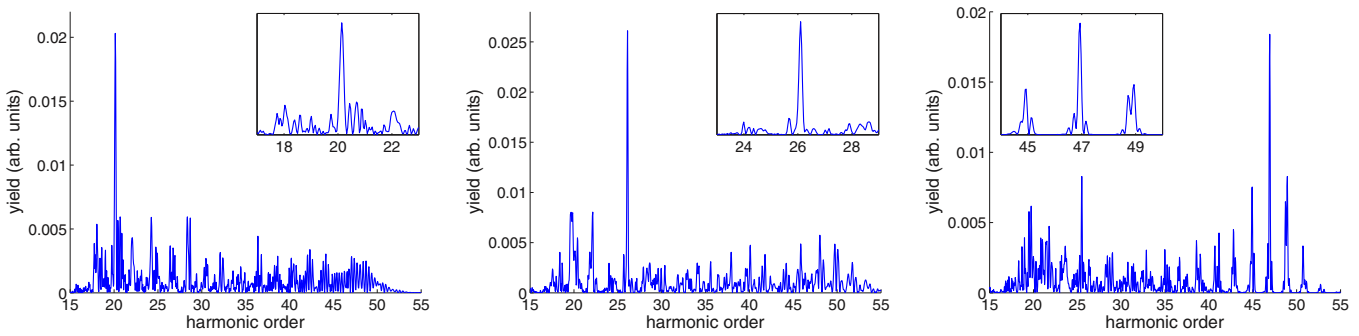

FIG. 1. (Color online) Harmonic spectra selectively enhancing H20 (left), H26 (center), and H47 (right). The inset of each panel zooms in the target harmonic with its nearest neighbors. A two-color field (800 nm + 267 nm) has been used. The three spectra are obtained using the same intensity but different relative phases and chirp rates.

we are interested in generating a harmonic spectrum that is dominated by a single harmonic order: We want the desired harmonic order to be as strong as possible and at the same time all other harmonic orders as weak as possible.

It is difficult to tell in advance which parameter combination will work for our purpose and which will work best. Instead, we *search* for the parameter combinations that meet our requirements.

We use a genetic algorithm (GA) [33] to do the search. GA is a search heuristic that mimics the process of natural selection and has been widely used in search or optimization problems. We use a micro-GA algorithm with a population of five in each generation, and let the evolution run for 10 000 generations to guarantee convergence. The procedure of searching for a parameter combination that selectively enhances a target harmonic order, say the Nth order, is listed as follows:

(1) We locate *the highest peak* of the harmonic spectrum generated by a laser field characterized by a parameter combination $(\alpha_1,\alpha_2,\phi_2)$ and require that this peak is within a small order range $[N-0.5,N+0.5]$. Of course, most parameter combinations do not meet this requirement and they will be given a bad fitness value (i.e., a bad evaluation) and eliminated. Only those parameter combinations that do meet this requirement will pass their gene to the next generation.

(2) We look for a parameter combination that optimizes the target harmonic order and at the same time suppresses all other harmonic orders. So we search for a parameter combination that maximizes *the ratio between the highest peak and the second highest peak* of the harmonic spectrum. Given step (1), the highest peak must be within the range $[N-0.5,N+0.5]$. There is no restriction for the position of the second highest peak.

We will also be interested in selectively enhancing two harmonic orders of interest, say the N_1th order and the N_2th order. The search procedure is an extension to the one introduced above, as listed below:

(1) We locate the *first two highest peaks* of the harmonic spectrum generated by a laser field characterized by $(\alpha_1,\alpha_2,\phi_2)$ and require that one of the peaks lies within $[N_1-0.5,N_1+0.5]$ and the other within $[N_2-0.5,N_2+0.5]$. Most parameter combinations do not meet this requirement and they will be given a bad fitness value and eliminated. Only those parameter combinations that meet this requirement will pass their gene to the next generation.

(2) We look for a parameter combination that maximizes the first two highest peaks and at the same time suppresses all other harmonic orders. So we search for a parameter combination that optimizes *the ratio between the second highest peak and the third highest peak*. Given the previous step (1), the position of the second highest peak is either within $[N_1-0.5,N_1+0.5]$ or within $[N_2-0.5,N_2+0.5]$. There is no restriction for the position of the third highest peak.

III. RESULTS AND ANALYSES

A. Selective enhancement of a single harmonic

We first demonstrate that it is possible to find parameter combinations $(\alpha_1,\alpha_2,\phi_2)$ to selectively enhance a single harmonic order. For example, Fig. 1 shows three harmonic spectra that selectively enhance three different harmonic orders (H20, H26, and H47, respectively) ranging across almost the whole spectral range. Each target harmonic stands out prominently from the background. The insets zoom in the target harmonics with their neighbors. A contrast ratio about five times can be found in the first case between the target harmonic and its nearest neighbors. The contrast ratio is about ten times in the second case and over two times in the third case.

The target atom is Ne. The laser consists of an 800 nm fundamental field of peak intensity 3×10^{14} W/cm^2 and its third harmonic, a 267 nm field of peak intensity 1.5×10^{13} W/cm^2, 5% of the fundamental. As explained above, we choose this intensity ratio because it is close to the intensity conversion efficiency of a BBO crystal in generating tird harmonics. The two fields share the same ten-cycle (FWHM, about 27 fs) cosine-square pulse envelope, in terms of the fundamental field.

All three spectra shown in Fig. 1 were obtained using the same field intensities but different parameters $(\alpha_1,\alpha_2,\phi_2)$. The parameter combinations for the three panels of Fig. 1 are listed in the following table:

	α_1 (10^{-5} a.u.)	α_2 (10^{-5} a.u.)	ϕ_2 (rad)
Fig. 1 (left)	0.485	0.281	0.860
Fig. 1 (center)	0.664	−1.844	0.541
Fig. 1 (right)	0.203	−1.858	1.183

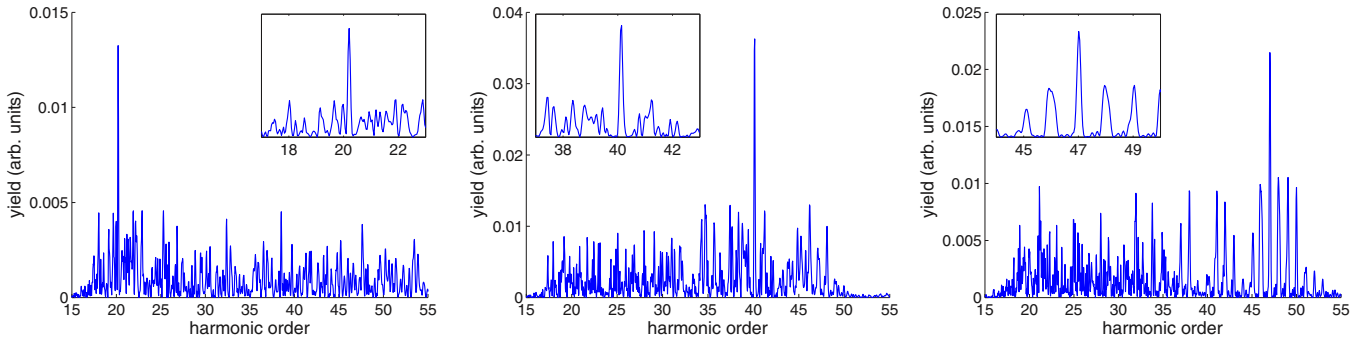

FIG. 2. (Color online) Harmonic spectra selectively enhancing H20 (left), H40 (center), and H47 (right) using 400 nm as the second color. The inset of each panel zooms in the target harmonic with its nearest neighbors. The three spectra are obtained using the same intensities but different relative phases and chirp rates.

Note that we have used atomic units for the chirp rates and radians for the phase delay.

Selective enhancement of a single harmonic order does not have to be limited to the (800 nm + 267 nm) configuration. Similar control goals can also be achieved using other two-color configurations. For example, Fig. 2 shows examples of selective single harmonic enhancement using 400 nm as the second color. Similar to the examples shown in Fig. 1, a single harmonic order can be selectively enhanced from almost the whole high-harmonic spectral range with good contrast ratios.

We have used the same target atom (Ne). The peak intensity of the 800 nm field is also set to be 3×10^{14} W/cm^2. The peak intensity of the 400 nm field is 4.5×10^{13} W/cm^2, 15% of the fundamental. As explained, this intensity ratio is used because it is close to the intensity conversion efficiency of a BBO crystal in generating second harmonics. The two fields share the same ten-cycle cosine-square pulse envelope.

The parameter combinations (α_1,α_2,ϕ_2) for the three panels of Fig. 2 are listed in the following table:

	α_1 (10^{-5} a.u.)	α_2 (10^{-5} a.u.)	ϕ_2 (rad)
Fig. 2 (left)	0.840	1.490	4.176
Fig. 2 (center)	−0.525	1.969	4.712
Fig. 2 (right)	0.151	−0.750	4.718

B. Analyses

To understand the mechanism of selective single harmonic enhancement, we take the third case of Fig. 1 as an example, which selectively enhances a frequency in the XUV regime (47th order, about 73 eV). The left panel of Fig. 3 (solid blue curve) shows the center part of the laser electric field that generates this spectrum, together with its chirp-free counterpart (dashed red curve) for the purpose of comparison. One can see that the blue curve is fairly moderately chirped: Strong chirp rates are not required for the purpose of selective harmonic enhancement. The right panel compares the harmonic spectra generated from these two laser fields. The chirp-optimized field enhances the target harmonic for about 30 times compared to the chirp-free field, without substantially increasing the total ionization probability (which increases from 0.5% to 0.6% according to the Ammosov-Delone-Krainov theory [34]).

To find out the origin of this enhancement, we have performed a time-frequency analysis [11,35] for the target order, for both the chirp-optimized case and the corresponding chirp-free case. We choose the Morlet wavelet and the transform reads

$$d_\omega(t) = \sqrt{\frac{\omega}{\tau}} \int d(t') e^{-\omega^2 (t'-t)^2 / 2\tau^2} e^{i\omega(t'-t)} dt', \qquad (8)$$

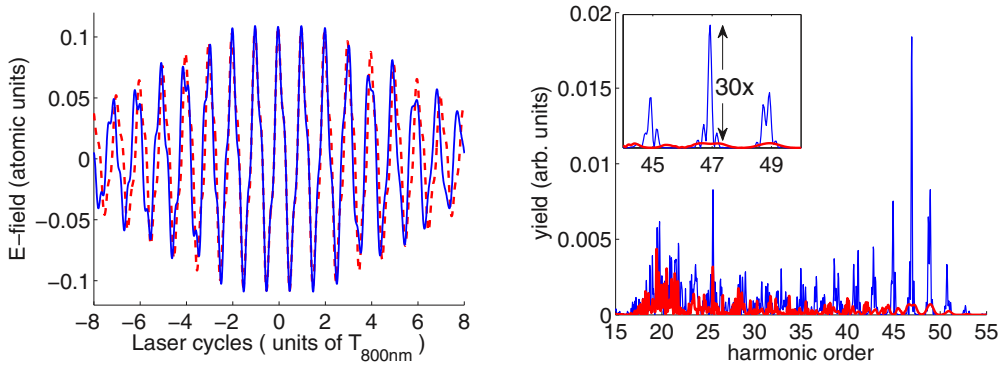

FIG. 3. (Color online) Left: The solid blue curve shows the center part of the laser electric field that generates the harmonic spectrum shown in the right panel of Fig. 1 and the dashed red curve shows the corresponding field without chirp for the purpose of comparison. Right: The harmonic spectra generated from these two laser fields. The inset zooms in the target harmonic order selected to be enhanced. An enhancement of 30 times has been obtained for H47.

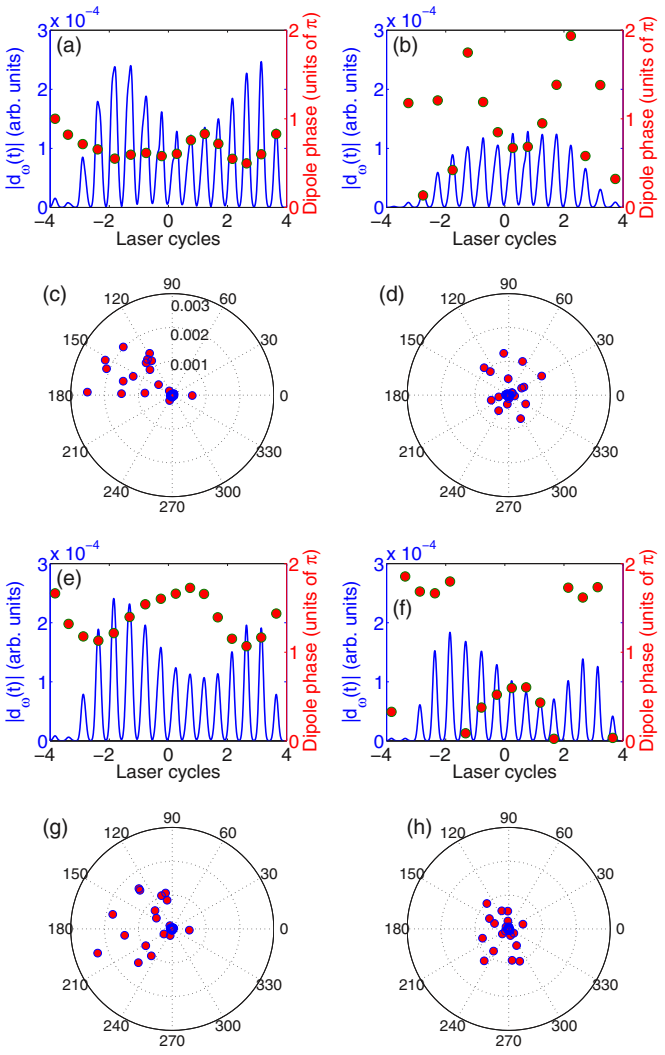

FIG. 4. (Color online) (a),(b) Wavelet analysis for H47: time profile (blue) and the corresponding dipole phases at the peaks (red circles) for the chirp-optimized laser field (a) and for the chirp-free laser field (b). (c),(d) Contributions from different half cycles to H47: for the chirp-optimized laser field (c) and for the chirp-free laser field (d). Each circle corresponds to a half-cycle contribution. A total number of 50 half cycles are included, although most of them have small amplitudes and cannot be visually distinguished from the center of the polar plots. (e),(g) Wavelet analysis and half-cycle analysis for H49. (f),(h) Wavelet analysis and half-cycle analysis for H51. All polar plots use the same radial scale.

where $d(t')$ is the dipole moment obtained from SFA [31], $\omega = 2.68$ a.u. is the frequency corresponding to H47, and τ is the width of the time window. Here we choose $\tau = 18$ a.u. which is about 1/6 of the fundamental (800 nm) field cycle duration.

The complex value $d_\omega(t)$ can be written as $|d_\omega(t)| \exp[i\theta(t) - i\omega t]$. The amplitude part, which is usually called a time profile, has been plotted in Figs. 4(a) and 4(b) as blue curves, for the chirp-optimized field and the chirp-free field, respectively. The time profile can be classically understood as the time of recollision [36,37], or the time of harmonic emission. For both cases, one can find two emission peaks per cycle, as expected. The important part in the phase is the dipole phase $\theta(t)$, which tells the temporal coherency between different emission times (recollision events). The dipole phases at the peaks of the time profiles are shown in Figs. 4(a) and 4(b) as red circles.

From the time profiles and the dipole phases, we can find two reasons why the chirp-optimized field can greatly enhance the target harmonic order compared to its chirp-free counterpart. First, the time profile amplitude for the chirp-optimized field is stronger than that for the chirp-free field (by roughly a factor of 2 in some time regions). Second and more important, the dipole phases are arranged in order for the chirp-optimized field. As can be seen from Fig. 4, the dipole phases at the time profile peaks are all confined within a range of about $\pi/2$ for the chirp-optimized field, whereas they are randomly scattered for the chirp-free field. Therefore in the chirp-optimized case, different emission times have better temporal coherence and they add constructively to generate a strong harmonic at the target frequency. Both the above harmonic enhancing channels are the consequences of laser field microshaping by chirps.

We have also performed another analysis without involving wavelet transform. As we know, a harmonic spectrum is the result of a coherent contribution from all laser cycles, or laser half cycles. We trace back all the half-cycle contributions for the target harmonic by dividing the laser field into half cycles according to zero field crossings and separating out contributions from different half cycles. For any given harmonic order, each half cycle contributes in the form of a complex number. The polar-plane distribution of these complex numbers for the target harmonic order is shown in Figs. 4(c) and 4(d), for the chirp-optimized field and the chirp-free field, respectively. One sees that for the chirp-optimized field, almost all the half-cycle contributions are confined within a narrow angle range between 120° and 180°. Whereas for the chirp-free field, the half-cycle contributions are quite randomly distributed in angle. This simple half-cycle analysis is consistent to the above wavelet analysis: The chirp-optimized field aligns the phase of different half-cycle contributions and also to some extent increases the absolute contributions of some half cycles.

We know that for an infinite (continuous-wave) monochromatic field (or a superposition of ω and 3ω, no matter what phase delay between them), the laser field repeats itself every half cycle in alternating directions. This half-cycle periodicity is the reason why all the odd harmonics build up and all the even harmonics cancel out. For an infinite pulse, it is not possible to further enhance any odd harmonic because all the half-cycle contributions are optimally in phase. However, this optimal in-phase or coherent property can be lost for a real pulse with finite duration, even if the duration is not very short. This point can be clearly seen in Figs. 4(b) and 4(d). Applying proper chirps to a finite laser pulse can to a good extent compensate the coherency loss and this is exactly the reason for the harmonic enhancement.

The temporal coherence optimized for a particular harmonic order (H47 here) degrades quickly with the change of harmonic orders. For example, panels (e) and (g) of Fig. 4 show the wavelet analysis and the half-cycle analysis for H49, two orders away from the optimized order of H47. Comparing panels (e) and (a), one sees that the nice dipole

phase alignment in (a), especially for high time-profile peaks, is largely lost in (e). And this loss of phase alignment, or temporal coherence, can be seen more obviously in panel (f) for H51, another two orders away. The same trend can be seen by comparing panels (c), (g), and (h) from half-cycle analyses. This phase misalignment, or loss of temporal coherence, is responsible for the sharp decrease in harmonic yield from H47 to H51, observing that the time-profile amplitudes do not change substantially. The high sensitivity of the temporal coherence on harmonic order makes it possible to selectively enhance a single harmonic order of interest.

C. Selective enhancement of two harmonics

We further show that a simple two-color-linear-chirp combination is able to obtain new harmonic control options, such as selectively enhancing two harmonic orders of interest. Figure 5 shows two examples. The left panel shows selective enhancement of H19 and H21 and the right panel shows selective enhancement of H22 and H26.

Figure 5 was obtained using an 800 nm field of peak intensity 3×10^{14} W/cm^2 and its third harmonic of peak intensity 1.5×10^{13} W/cm^2, the same intensities as used in Fig. 1. The parameter combinations $(\alpha_1,\alpha_2,\phi_2)$ are also searched using GA and the detailed search procedure has been explained in Sec. II C.

The parameter combinations $(\alpha_1,\alpha_2,\phi_2)$ for the two panels of Fig. 5 are listed in the following table:

	α_1 (10^{-5} a.u.)	α_2 (10^{-5} a.u.)	ϕ_2 (rad)
Fig. 5 (left)	−0.211	1.123	4.892
Fig. 5 (right)	0.626	0.219	0.233

IV. EXTENDING TO THREE COLORS AND CONNECTION TO A RECENT EXPERIMENT

The combination between single-color phase shaping and multicolor amplitude synthesis is of course not limited to the simplest two-color version that has been used above, although the harmonic control power of this simplest version has been demonstrated. Next we go one step further by adding a third color into the current configuration, mainly for the purpose of connecting to a recent experiment [19].

In the experiment a fundamental 800 nm field and its second (400 nm) and third (267 nm) harmonics are used. The 800 nm field and the 267 nm field are polarized in parallel, but the 400 nm field is perpendicularly polarized to the other two fields. Both the second and third harmonics are generated using BBO crystals. The intensity of the second harmonic is about 15% of the fundamental and the intensity of the third harmonic is about 5% of the fundamental.

The experiment was done with Ar, instead of Ne that has been used in this paper above. To compare with the experiment and also to demonstrate that our analysis above is applicable to different gas targets, we switch to Ar and use the same three-color configuration as used in the experiment. The laser electric field has the following form:

$$\begin{aligned}\mathbf{E}(t) = \cos^2(\pi t/\tau)[&\hat{\mathbf{e}}_{\mathbf{x}} E_1 \cos(\omega_1 t + \alpha_1 t^2) \\ &+ \hat{\mathbf{e}}_{\mathbf{y}} E_2 \cos(\omega_2 t + \alpha_2 t^2 + \phi_2) \\ &+ \hat{\mathbf{e}}_{\mathbf{x}} E_3 \cos(\omega_3 t + \alpha_3 t^2 + \phi_3)], \end{aligned} \quad (9)$$

where the subscript number 1 denotes the fundamental field, number 2 denotes the second harmonic field, and number 3 denotes the third harmonic field. Respectively, α_i and ϕ_i are the linear chirp rate and the phase delay of the ith field.

To be able to compare with the experiment, macroscopic propagation effects must be taken into account. We use an intensity-averaging method that has been shown to be an accurate approximation to real propagation results for a gas-jet setup, which is the setup used in the experiment, if the gas jet is placed behind the laser focus [38]. For each intensity I_0, we calculate the harmonic spectra corresponding to a range of intensities around I_0, and sum all these spectra *coherently*. In our calculation, an intensity range $[0.95I_0, 1.05I_0]$ has been used. We have checked other intensity ranges and our discussion is not affected.

In the experimental paper, the authors show selective enhancement of H14 at intensity about 1.2×10^{14} W/cm^2 and selective enhancement of H18 at intensity about 2.0×10^{14} W/cm^2 [see Fig. 3(c) of Ref. [19]]. In Fig. 6, we show numerical results that selectively enhance H14 (left panel) and H18 (right panel). To obtain a better contrast, in the H18 case we have used a slightly higher intensity of 2.5×10^{14} W/cm^2. One can see that selective enhancement of a single harmonic is clearly seen even after intensity averaging (propagation). Thus our theory provides a qualitative explanation to the experiment.

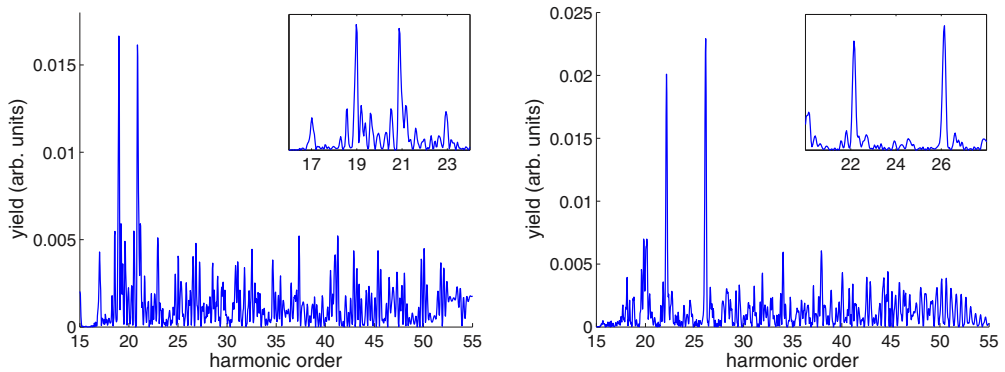

FIG. 5. (Color online) Selective enhancement of two harmonic orders of interest. Left: Selective enhancement of H19 and H21. Right: Selective enhancement of H22 and H26. Inset of each panel zooms in a small spectral region around the target harmonic orders.

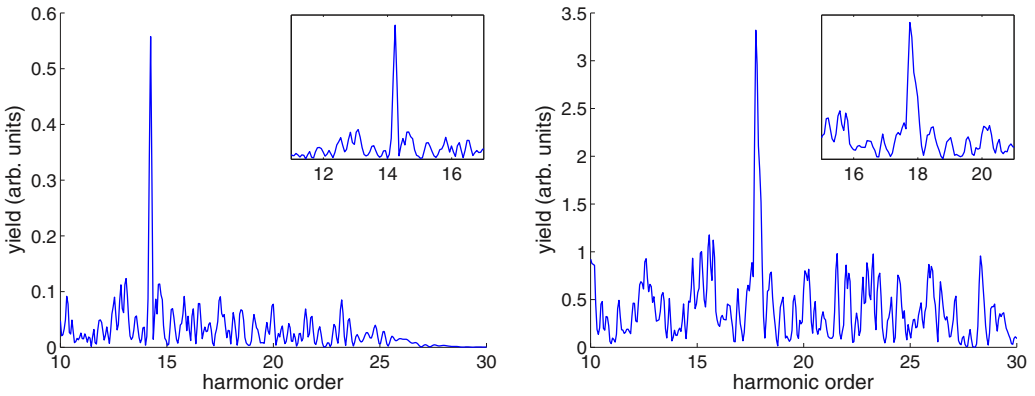

FIG. 6. (Color online) Intensity-averaged harmonic spectra that selectively enhance (left) H14 with a fundamental intensity of 1.2×10^{14} W/cm^2, and (right) H18 with a fundamental intensity of 2.5×10^{14} W/cm^2. Insets zoom in the target harmonics.

The laser parameter values for Fig. 6 are listed in the following table:

	$\alpha_1(10^{-5}$ a.u.)	$\alpha_2(10^{-5}$ a.u.)	$\alpha_3(10^{-5}$ a.u.)
Fig. 6 (left)	1.113	1.795	2.499
Fig. 6 (right)	−2.298	3.000	−1.108
	ϕ_2 (rad)	ϕ_3 (rad)	
Fig. 6 (left)	4.311	1.578	
Fig. 6 (right)	1.022	5.667	

V. SUMMARY

In summary, there are two current techniques of coherent harmonic control, namely, single-color phase shaping and multicolor amplitude synthesis. We suggest the possibility of combining the two techniques to achieve better harmonic control for some control purposes. Two simplest versions of this suggested combination have been considered, by using two colors or three colors and allowing a linear chirp for each color.

We find that a single harmonic (or two harmonic orders) can be selectively enhanced by just using these simplest combinations. Contrast ratios about an order of magnitude can be achieved in some cases between the target harmonic and its neighbors. Harmonic orders from a wide spectral range can be selectively enhanced by adjusting only a few parameters and the laser field maintains a simple analytical form.

Two analyzing methods have been used and they provide consistent physical insights. One is time-frequency analysis and the other is half-cycle analysis. A properly chirped two-color field is found to optimize the temporal coherence of different half cycles.

Our theory provides a qualitative explanation to a recently published experiment [19]. As efficient tools for coherent harmonic control, waveform-synthesized chirped laser fields are well within the scope of current experimental technology.

ACKNOWLEDGMENTS

The authors thank Dr. Zhinan Zeng of Shanghai Institute of Optics and Fine Mechanics for communications about their experiment. The authors acknowledge Dr. A. T. Le and Chao Yu for helpful discussions. This research was supported by Chemical Sciences, Geosciences and Biosciences Division, Office of Basic Energy Sciences, Office of Science, U.S. Department of Energy.

[1] C. Spielmann, N. H. Burnett, S. Sartania, R. Koppitsch, M. Schnurer, C. Kan, M. Lenzner, P. Wobrauschek, and F. Krausz, Science **278**, 661 (1997).
[2] A. Rundquist, C. G. Durfee, Z. H. Chang, C. Herne, S. Backus, M. M. Murnane, and H. C. Kapteyn, Science **280**, 1412 (1998).
[3] P. M. Paul, E. S. Toma, P. Breger, G. Mullot, F. Auge, P. Balcou, H. G. Muller, and P. Agostini, Science **292**, 1689 (2001).
[4] M. Hentschel, R. Kienberger, Ch. Spielmann, G. A. Reider, N. Milosevic, T. Brabec, P. Corkum, U. Heinzmann, M. Drescher, and F. Krausz, Nature (London) **414**, 509 (2001).
[5] Y. Mairesse, A. de Bohan, L. J. Frasinski, H. Merdji, L. C. Dinu, P. Monchicourt, P. Breger, M. Kovačev, R. Taïeb, B. Carré, H. G. Muller, P. Agostini, and P. Salières, Science **302**, 1540 (2003).
[6] C. Winterfeldt, C. Spielmann, and G. Gerber, Rev. Mod. Phys. **80**, 117 (2008).
[7] R. Bartels, S. Backus, E. Zeek, L. Misoguti, G. Vdovin, I. P. Christov, M. M. Murnane, and H. C. Kapteyn, Nature (London) **406**, 164 (2000).
[8] R. Bartels, S. Backus, I. P. Christov, H. C. Kapteyn, and M. M. Murnane, Chem. Phys. **267**, 277 (2001).
[9] D. H. Reitze, S. Kazamias, F. Weihe, G. Mullot, D. Douillet, F. Augé, O. Albert, V. Ramanathan, J. P. Chambaret, D. Hulin, and P. Balcou, Opt. Lett. **29**, 86 (2004).
[10] D. Walter, T. Pfeiffer, C. Winterfeldt, R. Kemmer, R. Spitzenpfeil, G. Gerber, and C. Spielmann, Opt. Express **14**, 3433 (2006).
[11] X. Chu and Shi-I. Chu, Phys. Rev. A **64**, 021403(R) (2001).
[12] T. Baumert, T. Brixner, V. Seyfried, M. Strehle, and G. Gerber, Appl. Phys. B **65**, 779 (1997).
[13] A. Wirth *et al.*, Science **334**, 195 (2011).

[14] S. Watanabe, K. Kondo, Y. Nabekawa, A. Sagisaka, and Y. Kobayashi, Phys. Rev. Lett. **73**, 2692 (1994).
[15] I. J. Kim, C. M. Kim, H. T. Kim, G. H. Lee, Y. S. Lee, J. Y. Park, D. J. Cho, and C. H. Nam, Phys. Rev. Lett. **94**, 243901 (2005).
[16] J. Mauritsson, P. Johnsson, E. Gustafsson, A. L'Huillier, K. J. Schafer, and M. B. Gaarde, Phys. Rev. Lett. **97**, 013001 (2006).
[17] L. E. Chipperfield, J. S. Robinson, J. W. G. Tisch, and J. P. Marangos, Phys. Rev. Lett. **102**, 063003 (2009).
[18] L. Brugnera, D. J. Hoffmann, T. Siegel, F. Frank, A. Zaïr, J. W. G. Tisch, and J. P. Marangos, Phys. Rev. Lett. **107**, 153902 (2011).
[19] P. Wei, J. Miao, Z. Zeng, C. Li, X. Ge, R. Li, and Z. Xu, Phys. Rev. Lett. **110**, 233903 (2013).
[20] P. Wei, Z. Zeng, J. Jiang, J. Miao, Y. Zheng, X. Ge, C. Li, and R. Li, Appl. Phys. Lett. **104**, 151101 (2014).
[21] F. Brizuela, C. M. Heyl, P. Rudawski, D. Kroon, L. Rading, J. M. Dahlström, J. Mauritsson, P. Johnsson, C. L. Arnold, and A. L'Huillier, Sci. Rep. **3**, 1410 (2013).
[22] C. Jin, G. Wang, H. Wei, A.-T. Le, and C. D. Lin, Nat. Commun. **5**, 4003 (2014).
[23] C. Vozzi, F. Calegari, F. Frassetto, L. Poletto, G. Sansone, P. Villoresi, M. Nisoli, S. De Silvestri, and S. Stagira, Phys. Rev. A **79**, 033842 (2009).
[24] E. J. Takahashi, P. Lan, O. D. Mücke, Y. Nabekawa, and K. Midorikawa, Phys. Rev. Lett. **104**, 233901 (2010).
[25] T. Siegel *et al.*, Opt. Express **18**, 6853 (2010).
[26] H.-C. Bandulet, D. Comtois, E. Bisson, A. Fleischer, H. Pépin, J.-C. Kieffer, P. B. Corkum, and D. M. Villeneuve, Phys. Rev. A **81**, 013803 (2010).
[27] S. Huang *et al.*, Nat. Photonics **5**, 475 (2011).
[28] E. J. Takahashi, P. Lan, O. D. Mücke, Y. Nabekawa, and K. Midorikawa, Nat. Commun. **4**, 2691 (2013).
[29] S. Haessler *et al.*, Phys. Rev. X **4**, 021028 (2014).
[30] X. Liu and C. Figueira de Morisson Faria, Phys. Rev. Lett. **92**, 133006 (2004).
[31] M. Lewenstein, Ph. Balcou, M. Yu. Ivanov, A. L'Huillier, and P. B. Corkum, Phys. Rev. A **49**, 2117 (1994).
[32] A.-T. Le, R. R. Lucchese, S. Tonzani, T. Morishita, and C. D. Lin, Phys. Rev. A **80**, 013401 (2009).
[33] D. L. Carroll, FORTRAN genetic algorithm driver, version 1.7a, 2001, http://cuaerospace.com/carroll/ga.html.
[34] M. V. Ammosov, N. B. Delone, and V. P. Krainov, Sov. Phys. JETP **64**, 1191 (1987).
[35] P. Antoine, B. Piraux, and A. Maquet, Phys. Rev. A **51**, R1750 (1995).
[36] P. B. Corkum, Phys. Rev. Lett. **71**, 1994 (1993).
[37] K. J. Schafer, B. Yang, L. F. DiMauro, and K. C. Kulander, Phys. Rev. Lett. **70**, 1599 (1993).
[38] C. Jin, A. T. Le, and C. D. Lin, Phys. Rev. A **79**, 053413 (2009).